Chirality of the gravitational-wave background and pulsar-timing arrays

Enis Belgacem[1, *] and Marc Kamionkowski[2, †]

[1]*Département de Physique Théorique and Center for Astroparticle Physics,*
Université de Genève, 24 quai Ansermet, CH–1211 Genève 4, Switzerland
[2]*Department of Physics and Astronomy, Johns Hopkins University,*
3400 N. Charles St., Baltimore, MD 21218, USA

We describe the signatures of a circularly polarized gravitational-wave background on the timing residuals obtained with pulsar-timing arrays. Most generally, the circular polarization will depend on the gravitational-wave direction, and we describe this angular dependence in terms of spherical harmonics. While the amplitude of the monopole (the overall chirality of the gravitational-wave background) cannot be detected, measures of the anisotropy are theoretically conceivable. We provide expressions for the minimum-variance estimators for the circular-polarization anisotropy. We evaluate the smallest detectable signal as a function of the signal-to-noise ratio with which the isotropic GW signal is detected and the number of pulsars (assumed to be roughly uniformly spread throughout the sky) in the survey. We find that the overall dipole of the circular polarization and a few higher overall multipoles, are detectable in a survey with $\gtrsim 100$ pulsars if their amplitude is close to maximal and once the isotropic signal is established with a signal-to-noise ratio $\gtrsim 400$. Even if the anisotropy can be established, though, there will be limited information on its direction. Similar arguments apply to astrometric searches for gravitational waves.

I. INTRODUCTION

A gravitational wave passing between the Earth and a pulsar is known to affect the periodicity of the observed pulses [1, 2]. The effect can be encoded in the timing residual, defined as the relative difference between the observed period of pulses and the one produced by the pulsar. The explorable frequency range roughly goes from a few nHz to 1 μHz, the lower limit being determined by the time span of observations and the upper limit by the data sampling rate. Monitoring and correlating the irregularities in the signals emitted by different pulsars allows an indirect study of gravitational waves (GWs) and has led to the idea of pulsar timing arrays (PTAs) [3–13] to detect gravitational waves at ∼nHz–μHz frequencies. In particular it may be possible to extract information on the stochastic gravitational-wave background due to supermassive-black-hole (SMBH) mergers [14, 15]. There are also prospects to augment PTA measurements with information from stellar astrometry [16–20].

A stochastic background from SMBH mergers may well be anisotropic, given the uneven distribution of SMBH mergers on the sky [21–25] and prior work [26–29] has developed tools to seek and characterize anisotropies in the intensity of the GW background with PTAs/astrometry. However, GWs from SMBH mergers will most generally be circularly polarized. Therefore, the stochastic GW background is likely to be circularly polarized, with an amplitude that varies across the sky. Ref. [30] discussed techniques to seek this circular polarization with PTAs.

In this paper we re-visit the PTA search for circular polarization with a simple augmentation of recent work [29] on the detection of angular GW-intensity fluctuations. Unlike most prior related work, Ref. [29] discussed angular fluctuations in harmonic space, rather than configuration space, an alternative approach that provides elegant/economical mathematical expressions, simple estimates for signal detectability, and some novel insights. Here, we show how that work is easily altered to allow a search for circular polarization. While the results are formally equivalent to what was presented in Ref. [30], the formalism here allows for more compact mathematical expressions and some associated insights.

Ref. [29] idealized measurements of a timing-residual $z(\hat{n}, t)$ as a function of position $\hat{n}$ on the sky and time t. The time dependence was then described in terms of its Fourier amplitudes for frequency f (one real amplitude for the sine, with respect to some nominal $t = 0$ time, and another for the cosine for each f), The resulting Fourier maps $z_f(\hat{n})$ were then decomposed in terms of spherical-harmonic coefficients $z_{f,\ell m}$. Estimators for angular intensity fluctuations were then constructed from bipolar spherical harmonics (BiPoSHs) [31–33], and in particular from BiPoSHs of even parity.

In this paper, estimators for the circular polarization of the GW background will be similarly constructed but with a few notable differences: First, a circularly polarized GW is a linear combination of two linear polarizations that are out of phase. Thus, a circular-polarization estimator requires that we consider the sine and cosine amplitudes *together* for any given frequency f, which we do here by allowing $z_f(\hat{n})$ to be complex. We then show that circular-polarization estimators look identical to those for intensity fluctuations, but for *odd*-parity (rather than even-parity) BiPoSHs [34].

The plan of the paper is as follows: We review in Section II the expansion of the timing residuals in terms of spherical harmonics and review the BiPoSH formalism that will be used to construct estimators for circular-

---
* enis.belgacem@unige.ch
† kamion@jhu.edu

polarization anisotropies. Section III presents the model we assume for the stochastic background and obtains predictions for the observables for this background. Section IV presents the estimators for the circular-polarization anisotropies, and formal expressions for the variances with which these estimators can be measured. Section V then presents quantitative results for the smallest detectable circular-polarization anisotropies, and concluding remarks are presented in Section VI.

II. SPHERICAL-HARMONIC EXPANSION AND BIPOLAR SPHERICAL HARMONICS (BIPOSHS)

We imagine a set of pulsars spread roughly uniformly across the sky so that the GW-induced timing residual $z(\hat{n}, t)$ can be obtained as a function of time t and position $\hat{n}$. The time sequence can then be represented equivalently in terms of the Fourier components $z_f(\hat{n})$ for frequency f, and the angular pattern can then be represented in terms of the spherical-harmonics components as

$$z_f(\hat{n}) = \sum_{\ell=0}^{\infty} \sum_{m=-\ell}^{L} z_{f,\ell m} Y_{\ell m}(\hat{n}). \quad (1)$$

In Ref. [29], it was presumed that $z_f(\hat{n})$ could be taken to be real: the intensity-fluctuation analysis therein could be performed independently on either the real or the imaginary part (or equivalently, on the amplitudes of the cosine or sine of any particular f mode). Thus, in that work (as in work on CMB temperature fluctuations), we had $z_{f,\ell m}^* = (-1)^m z_{f,\ell,-m}$. Put another way, the $2\ell + 1$ independent coefficients for any given ℓ could be taken to be $z_{f,\ell 0}$, the ℓ real parts $\sqrt{2}\,\mathrm{Re}\,z_{f,\ell m}$ of $z_{f,\ell m}$ for $m > 0$, and the ℓ imaginary components $\sqrt{2}\,\mathrm{Im}\,z_{f,\ell m}$ for $m > 0$.

For the analysis here, however, the complexity of $z_f(\hat{n})$—i.e., the relative amplitudes of the cosine and sine mode for a given f—is essential. Thus, in this paper, $z_f(\hat{n})$ is most generally complex, and so $z_{f,\ell m}^*$ is not necessarily equal to $(-1)^m z_{f,\ell m}$. For any given ℓ, there are now $2(2\ell + 1)$ components of $z_{f,\ell m}$ which can be taken to be the real and imaginary parts for all $-\ell \leq m \leq \ell$.

Also, for notational economy, we suppress below the subscripts f on the map, the spherical-harmonic coefficients, and power spectra. It should be understood that throughout the rest of the paper, it is assumed that the analysis is done for this one frequency component f. We then discuss in the Conclusions how to incorporate multiple frequencies.

A model for the stochastic background makes no predictions for the specific values of $z_{\ell m}$. Rather, it makes predictions for their correlations. The most general two-point correlation between any two $z_{\ell m}$ takes the form

(see, e.g., Refs. [34, 35]),

$$\langle z_{\ell m} z_{\ell' m'}^* \rangle = C_\ell \delta_{\ell \ell'} \delta_{mm'}$$
$$+ \sum_{L=1}^{\infty} \sum_{M=-L}^{L} (-1)^{m'} \langle \ell\, m\, \ell',\, -m' | LM \rangle A_{\ell \ell'}^{LM}, \quad (2)$$

where the $A_{\ell \ell'}^{LM}$ are bipolar spherical harmonics (BiPoSH) coefficients [31–33]. If the stochastic background is statistically isotropic and unpolarized, then $A_{\ell \ell'}^{LM} = 0$ for all $L \geq 1$. Ref. [29] found that anistropies in the intensity of the GW background resulted in nonzero BiPoSH coefficients of *even* parity (i.e., $L + \ell + \ell' =$even) only. We will see that circular polarization induces *odd*-parity BiPoSHs, those with $L + \ell + \ell' =$odd.

A. Estimators of BiPoSH coefficients

The measured timing-residual coefficients are assumed to be $z_{f,\ell m}^{\mathrm{data}} = z_{f,lm} + z_{f,\ell m}^{\mathrm{noise}}$ with

$$\langle z_{f,\ell m}^{\mathrm{noise}} z_{f,\ell' m'}^{*\,\mathrm{noise}} \rangle = N_f^{zz} \delta_{\ell \ell'} \delta_{mm'}, \quad (3)$$

with the noise power spectrum N_f^{zz} independent of ℓ (as will arise in the idealized scenario of pulsars distributed roughly uniformly on the sky, with comparable timing noises). The BiPoSH coefficients are estimated from data as

$$\widehat{A_{\ell \ell'}^{LM}} = \sum_{mm'} z_{lm}^{\mathrm{data}} z_{l'm'}^{*\,\mathrm{data}} (-1)^{m'} \langle l\, m\, l',\, -m' | LM \rangle. \quad (4)$$

The variance of this estimator was evaluated under the null hypothesis of a Gaussian and isotropic map, in Ref. [34]. That analysis assumed, however, a real map, whereas we are now taking $z(\hat{n})$ to be complex. As a result there is no requirement for $A_{\ell \ell'}^{LM}$ to be antisymmetric (for $L + \ell + \ell' =$odd) under $\ell \leftrightarrow \ell'$ nor for the $A_{\ell \ell}^{LM}$ to vanish for $\ell + \ell' + L =$odd. For a complex map and for $L + \ell + \ell' =$odd,

$$\left\langle \left| \widehat{A_{\ell \ell'}^{LM}} \right|^2 \right\rangle = C_\ell^{\mathrm{data}} C_{\ell'}^{\mathrm{data}}, \quad (5)$$

where $C_\ell^{\mathrm{data}} = C_\ell + N^{zz}$ includes both the signal and the noise power spectra.

The estimator for the isotropic power spectrum C_ℓ is

$$\widehat{C_\ell} = \sum_{m=-\ell}^{\ell} \frac{|z_{\ell m}^{\mathrm{data}}|^2}{2\ell + 1} - N^{zz}, \quad (6)$$

and its variance is

$$\left\langle (\Delta C_\ell)^2 \right\rangle = \frac{1}{2\ell + 1} \left(C_\ell^{\mathrm{data}} \right)^2. \quad (7)$$

Note that this expression differs from that, more commonly seen, for the case where $z(\hat{n})$ is real. As discussed above, in that case, each C_ℓ is estimated from the

$2\ell+1$ independent components of $z_{\ell m}$. If $z(\hat{n})$ is complex, though, then there are $2(2\ell+1)$ independent components of $z_{\ell m}$ yielding a replacement $2\ell+1 \to 2(2\ell+1)$ relative to the more familiar equation.

III.   A POLARIZED BACKGROUND AND ITS TIMING RESIDUALS

A.   Spherical-harmonic coeffcients

Eq. (18) in Ref. [29] provides the spherical-harmonic coefficients, induced by a single gravitational wave of frequency f propagating in the $\hat{k}$ direction. Identifying the GW circular-polarization amplitudes $h_R = 2^{-1/2}(h_+ + ih_\times)$ and $h_L = 2^{-1/2}(h_+ - ih_\times)$ in terms of the linear-polarization amplitudes h_+ and $h_\times$, that expression can be written [1]

$$z_{\ell m}(\hat{k}) = 2^{-1/2} z_\ell \left[h_L D_{m2}^{(\ell)} + h_R D_{m,-2}^{(\ell)} \right], \qquad (8)$$

where $D_{mm'}^{(\ell)}(\phi_k, \theta_k, 0)$ are the Wigner rotation functions specified by the three Euler angles ϕ_k, θ_k and $\psi_k = 0$ in the z-y-z convention, and

$$z_\ell \equiv (-1)^\ell \sqrt{\frac{4\pi(2\ell+1)(\ell-2)!}{(\ell+2)!}}. \qquad (9)$$

Only harmonics coefficients with $\ell \geq 2$ are generated in the timing residuals map.

The most general gravitational-wave background is then described by a superposition of plane waves propagating along any direction $\hat{k}$. The spherical-harmonic coefficients for this background are then

$$z_{\ell m}(\hat{k}) = 2^{-1/2} z_\ell \int \frac{d^3 k}{(2\pi)^3} \left[h_L(\vec{k}) D_{m2}^{(\ell)}(\vec{k}) + h_R(\vec{k}) D_{m,-2}^{(\ell)}(\vec{k}) \right], \qquad (10)$$

where we have summed over all GW wavevectors $\vec{k} = 2\pi f \hat{k}$.

B.   A circularly polarized gravitational-wave background

We now consider a gravitational-wave background described by the following wave-amplitude correlations:

$$\left\langle h_R(\vec{k}) h_R^*(\vec{k}') \right\rangle = \frac{1}{4}(2\pi)^3 \delta_D(\vec{k} - \vec{k}') P_h(k) \left[1 - \epsilon(\hat{k}) \right],$$

$$\left\langle h_L(\vec{k}) h_L^*(\vec{k}') \right\rangle = \frac{1}{4}(2\pi)^3 \delta_D(\vec{k} - \vec{k}') P_h(k) \left[1 + \epsilon(\hat{k}) \right],$$

$$\left\langle h_R(\vec{k}) h_L^*(\vec{k}') \right\rangle = 0. \qquad (11)$$

---

[1] We correct here a missing factor of two in Eqs. (14) and (15) of Ref. [29] (that does not affect the final quantitative results for anisotropy estimators presented there in terms of the signal-to-noise ratio SNR with which the isotropic signal is detected.)

The "chirality function" $\epsilon(\hat{k})$ is assumed to depend only on the direction of propagation, and it parametrizes the degree of circular polarization for GWs moving in direction $\hat{k}$. It can be decomposed in spherical harmonics as

$$\epsilon(\hat{k}) = \sum_{L=0}^{\infty} \sum_{M=-L}^{L} \epsilon_{LM} Y_{LM}(\hat{k}). \qquad (12)$$

Comparing to Eq. (13) of [29], where the index L is constrained to assume strictly positive values (i.e., $L \geq 1$), here the $L = 0$ term is in principle allowed because it cannot be reabsorbed into a redefinition of $P_h(k)$ for both the right-handed and left-handed power spectra in Eq. (11). However, we will see that the monopole gives no contribution to the correlators of timing residuals and is therefore not detectable.

Positivity of power spectra imposes the restrictions $\epsilon_{L0} \leq \sqrt{4\pi/(2L+1)}$ (with similar bounds for $\sqrt{2}\,\mathrm{Re}\,\epsilon_{LM}$ and $\sqrt{2}\,\mathrm{Im}\,\epsilon_{LM}$ for $M \neq 0$). The correlators between timing residual-coeffcients are then evaluated using Eq. (10) and are given by

$$\langle z_{\ell m} z_{\ell' m'}^* \rangle = \frac{1}{8} z_\ell z_{\ell'} \int \frac{d^3 k}{(2\pi)^3} P_h(k) \Bigg\{ D_{m2}^{(\ell)}(\hat{k}) \left(D_{m'2}^{(\ell')}(\hat{k}) \right)^*$$

$$\times \left[1 + \sum_{LM} \epsilon_{LM} Y_{LM}(\hat{k}) \right] + D_{m,-2}^{(\ell)}(\hat{k}) \left(D_{m',-2}^{(\ell')}(\hat{k}) \right)^*$$

$$\times \left[1 - \sum_{LM} \epsilon_{LM} Y_{LM}(\hat{k}) \right] \Bigg\}.$$

The integration over directions $\hat{k}$ leads to correlators of the form in Eq. (2) with

$$C_\ell = \frac{z_\ell^2}{4(2\ell+1)} I, \qquad (13)$$

and

$$A_{\ell\ell'}^{LM} = \frac{1 - (-1)^{\ell+\ell'+L}}{2}(-1)^{\ell-\ell'}(4\pi)^{-1/2} \epsilon_{LM} \frac{1}{4} z_\ell z_{\ell'} H_{\ell\ell'}^L I, \qquad (14)$$

where

$$H_{\ell\ell'}^L \equiv \begin{pmatrix} \ell & \ell' & L \\ 2 & -2 & 0 \end{pmatrix}, \qquad (15)$$

and $I \equiv [4\pi/(2\pi)^3] \int k^2 \, dk \, P_h(k)$.

The coefficient $\left[1 - (-1)^{\ell+\ell'+L} \right]/2$ selects only odd-parity BiPoSHs (odd values of $\ell + \ell' + L$). Comparing to Eq. (22) of Ref. [29] and the discussion therein, we see that the correlations induced by circular-polarization anisotropies differ from those of intensity anisotropies in the parity of the BiPoSHs allowed (odd for circular polarization and even for intensity). The other difference is that $A_{\ell\ell'}^{LM}$ is not degenerate here with $A_{\ell'\ell}^{LM}$ (as it is for the intensity estimator), as $z(\hat{n})$ here is taken to be the complex sum of the amplitudes of the sine and cosine of the frequency f.

IV. CHIRALITY ESTIMATORS

Estimators for the chirality coefficients ϵ_{LM} are obtained in direct analogy with Ref. [29] for a survey parametrized by the signal-to-noise ratio (SNR) with which the isotropic GW background is detected and the maximum multipole moment $\ell_{\max}$ (which is $\ell_{\max} \sim \sqrt{N_p}$ for a sky map with N_p pulsars distributed roughly uniformly on the sky) accessible with the survey. The SNR is obtained by summing in quadrature the SNRs for each accessible multipole ℓ, assuming an error on C_ℓ given by Eq. (7) with $C_\ell^{\rm data} = N^{zz}$, corresponding to the null hypothesis of no gravitational-wave background. The resulting SNR for the frequency channel f is [29, 36] (noting the extra factor of 2 for the complexity of $z(\hat{n})$),

$$\mathrm{SNR} = \left[\sum_{\ell=2}^{\ell_{\max}} (2\ell+1) \left(\frac{C_\ell}{N^{zz}} \right)^2 \right]^{1/2} \simeq \frac{\pi I}{6\sqrt{3}N^{zz}}. \quad (16)$$

The approximation holds for any $\ell_{\max}$ given that the sum is dominated very heavily by the lowest-ℓ terms.

Following the analysis in Ref. [29], the minimum-variance estimator for each chirality amplitude ϵ_{LM} is

$$\widehat{\epsilon_{LM}} = \frac{\sum_{\ell\ell'} (\widehat{\epsilon_{LM}})_{\ell\ell'} (\Delta\epsilon_{LM})_{\ell\ell'}^{-2}}{\sum_{\ell\ell'} (\Delta\epsilon_{LM})_{\ell\ell'}^{-2}}, \quad (17)$$

where

$$(\widehat{\epsilon_{LM}})_{\ell\ell'} = (-1)^{\ell-\ell'} 4\sqrt{4\pi} \frac{\widehat{A_{\ell\ell'}^{LM}}}{z_\ell z_{\ell'} H_{\ell\ell'}^L I}, \quad (18)$$

is the contribution of each $\ell\ell'$ pair to the estimator, and

$$(\Delta\epsilon_{LM})_{\ell\ell'}^2 = \frac{64\pi C_\ell^{\rm data} C_{\ell'}^{\rm data}}{(z_\ell z_{\ell'} H_{\ell\ell'}^L I)^2}$$
$$= \frac{16\pi^3}{27} \frac{C_\ell^{\rm data} C_{\ell'}^{\rm data}}{\left(z_\ell z_{\ell'} H_{\ell\ell'}^L\right)^2 (\mathrm{SNR})^2 (N^{zz})^2}, \quad (19)$$

is the variance of each of these contributions. The variance of the combined estimator $\widehat{\epsilon_{LM}}$ is then

$$(\Delta\epsilon_{LM})^{-2} = \sum_{\ell\ell'} (\Delta\epsilon_{LM})_{\ell\ell'}^{-2}. \quad (20)$$

It is independent of M. The ℓ, ℓ' sums here are over $\ell + \ell' + L$=odd. Since the $A_{\ell\ell'}^{LM}$ are not necessarily antisymmetric in ℓ, ℓ' (since $z(\hat{n})$ is not real here), the sums are over all ℓ, ℓ' pairs (not just those with $\ell' \geq \ell$ as in Ref. [29]).

Using Eqs. (13) and (16) we can express Eq. (20) in terms of the SNR for the detection of the isotropic unpolarized signal and, furthermore, the noise power spectrum N^{zz} cancels out from the final result, leaving us with

$$(\Delta\epsilon_{LM})^{-2} = \frac{27}{16\pi^3} \sum_{\ell\ell'} \left(z_\ell z_{\ell'} H_{\ell\ell'}^L \right)^2 \left(\frac{1}{\mathrm{SNR}} + \frac{3\sqrt{3}}{2\pi} \frac{z_\ell^2}{2\ell+1} \right)^{-1}$$
$$\times \left(\frac{1}{\mathrm{SNR}} + \frac{3\sqrt{3}}{2\pi} \frac{z_{\ell'}^2}{2\ell'+1} \right)^{-1}. \quad (21)$$

This expression can then be evaluated for any nominal SNR with which the isotropic signal is detected and taking the sums up to $\ell_{\max} \sim N_p^{1/2}$, with N_p the number of pulsars.

This expression evaluates, in the limit SNR $\to \infty$, to

$$(\Delta\epsilon_{LM})^{-2} \to \frac{1}{4\pi} \sum_{\ell\ell'} (2\ell+1)(2\ell'+1) \left(H_{\ell\ell'}^L \right)^2, \quad (22)$$

and in the limit SNR $\to 0$ to

$$(\Delta\epsilon_{LM})^{-2} \to \frac{27}{16\pi^3} \mathrm{SNR}^2 \sum_{\ell\ell'} \left(z_\ell z_{\ell'} H_{\ell\ell'}^L \right)^2. \quad (23)$$

V. RESULTS

A. Monopole is not observable

As anticipated in Section III, the monopole term ϵ_{00} is not observable. This is because the $L = M = 0$ BiPoSH coefficients, $A_{\ell\ell'}^{00} = (-1)^\ell \sqrt{2\ell+1} C_\ell$, all have $\ell = \ell'$ and therefore always have $L + \ell + \ell'$ =even. This agrees with a similar conclusion in Ref. [30] obtained using overlap reduction functions.

B. Dipole anisotropy

We now consider the lowest observable multipole, the dipole $L = 1$. Given the triangle constraint $|\ell - \ell'| \leq L$ and $\ell + \ell' + L$=odd, only $\ell = \ell'$ contributes to the sum. We then use $(H_{\ell\ell}^1)^2 = 4 \left[\ell(\ell+1)(2\ell+1) \right]^{-1}$ to obtain for the smallest detectable (at 3σ) signal,

$$\epsilon_{1M,\min} = 3\Delta\epsilon_{1M} = \frac{1}{2}\sqrt{\frac{\pi}{3}} \left\{ \sum_{\ell=2}^{\ell_{\max}} \frac{2\ell+1}{\left[(\ell+2)(\ell-1) \right]^2 \left[\ell(\ell+1) \right]^3} \right.$$
$$\left. \times \left[\frac{1}{\mathrm{SNR}} + 6\sqrt{3} \frac{(\ell-2)!}{(\ell+2)!} \right]^{-2} \right\}^{-1/2}. \quad (24)$$

We can understand this result analytically by considering the asymptotic behaviors in the limits of high and low signal-to-noise. When SNR $\to \infty$ and $\ell_{\max} \gg 1$ the sum in Eq. (24) converges to [2]

$$\epsilon_{1M,\min} \simeq \frac{3\sqrt{\pi}}{\sqrt{2\ln\ell_{\max} + 2\gamma_E - 5/2}}, \quad \text{as SNR} \to \infty. \quad (25)$$

In the low-SNR limit we find

$$\epsilon_{1M,\min} \simeq \frac{13.2}{\mathrm{SNR}}, \quad \text{as SNR} \to 0. \quad (26)$$

---

[2] Here, γ_E is Euler's constant and the finite correction $2\gamma_E - 5/2 \simeq -1.35$ is relevant as it gives a 13.6% correction on $\epsilon_{1M,\min}$ for $\ell_{\max} = 20$.
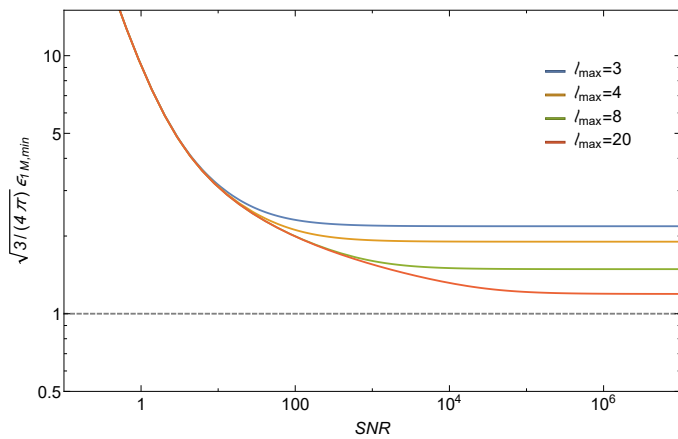
FIG. 1. The smallest detectable (at the 3σ level) circular-polarization dipole ϵ_{1M} (normalized to its maximum allowed value $\epsilon_{1M,\text{max}} = \sqrt{4\pi/3}$), as a function of the SNR with which the isotropic GW background is detected, for several values of the maximum timing-residual multipole moment ℓ_{max}.

Fig. 1 shows the smallest detectable dipole coefficient $\epsilon_{1M,\text{min}}$ as a function of the isotropic signal SNR, for a few values of ℓ_{max}. The value $(\text{SNR})_{\text{high}}$ at which $\epsilon_{1M,\text{min}}$ reaches its aymptotic value can be evaluated by looking at the second line of Eq. 24 and estimating the minimum value of SNR such that the addend $1/\text{SNR}$ can be neglected. This simple guess leads to [3]

$$(\text{SNR})_{\text{high}} \simeq \frac{(\ell_{\text{max}} + 2)!}{(\ell_{\text{max}} - 2)!}. \qquad (27)$$

The sensitivity of a PTA to a circular-polarization dipole is maximized once an SNR of this value is reached.

If we surmise (optimistically) an $\ell_{\text{max}} \simeq 20$ (corresponding to $N_p \sim 400$ pulsars), then Eq. (25) evaluates to $\epsilon_{1M,\text{min}} \simeq 2.5$, which is about 1.2 times the largest value, $\epsilon_{1M,\text{max}} = \sqrt{4\pi/3}$, that this amplitude can have. We thus conclude that an individual component ϵ_{1M} of the circular-polarization dipole is not detectable.

However, if we simply want to establish the existence of a circular-polarization dipole, without any constraint to its direction, we will evaluate the overall dipole amplitude,

$$d_c = \left[\sum_M |\epsilon_{1M}|^2 \right]^{1/2}. \qquad (28)$$

Since this is obtained as the sum, in quadrature, of the three ϵ_{1M}s, the smallest detectable d_c is about a factor of $\sqrt{3}$ smaller, implying (with $\ell_{\text{max}} \simeq 20$) that a dipole as small as 0.7 times the maximal dipole can actually be detected. If the local GW background, at the frequency

---

[3] The value of $\epsilon_{1M,\text{min}}$ at $(\text{SNR})_{\text{high}}$ differs from the true asymptotic value only by 1% for $\ell_{\text{max}} = 20$ and 5% for $\ell_{\text{max}} = 3$.

considered, is dominated by a single source or handful of sources, such a circular-polarization dipole is certainly conceivable and so worth seeking. On the other hand, the results discussed so far only hold for very large SNR, such that $\epsilon_{1M,\text{min}}$ reaches its asymptotic value (for example, when $\ell_{\text{max}} \simeq 20$, Eq. 27 gives $(\text{SNR})_{\text{high}} \simeq 1.8 \times 10^5$). For lower values of SNR there is less room for the observation of the dipole and one can establish numerically a threshold for the overall dipole detection. The corresponding minimal conditions for detection are a number of pulsars $N_p \gtrsim 100$ (i.e. $\ell_{\text{max}} \gtrsim 10$) and a very clear detection of the isotropic GW background with SNR $\gtrsim 400$. More precisely, for $\ell_{\text{max}} = 10$ and SNR = 400 only an overall dipole equal to 0.98 times the maximal value can be detected.

C. Other multipoles

Results for the detectability of higher order multipoles can be inferred by numerically evaluating the general expression in Eq. (21). Fig. 2 shows the smallest detectable multipole coefficients $\epsilon_{LM,\text{min}}$ (normalized to their maximum possible values $\epsilon_{LM,\text{max}} = \sqrt{4\pi/(2L+1)}$) as a function of the isotropic signal SNR, for several values of the multipole L and assuming $\ell_{\text{max}} = 20$.
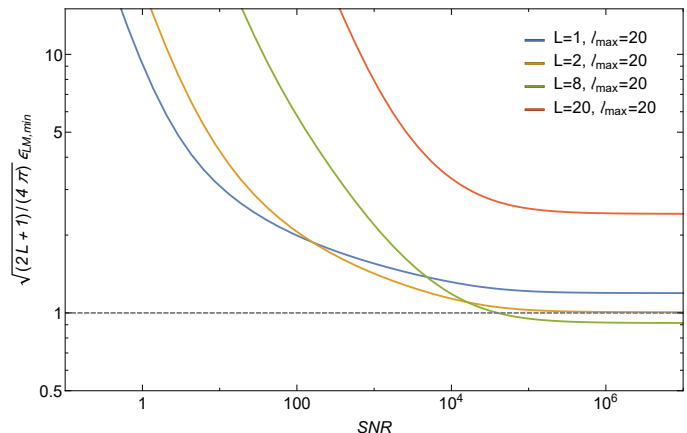

FIG. 2. The smallest detectable (at the 3σ level) circular-polarization multipoles ϵ_{LM} (normalized to their maximal values $\epsilon_{LM,\text{max}} = \sqrt{4\pi/(2L+1)}$), as a function of the SNR with which the isotropic GW background is detected, for several values of L and assuming a maximum timing-residual multipole moment $\ell_{\text{max}} = 20$.

The plot and the numerical analyis seem to imply that, for a given ℓ_{max}, some of the higher-order multipoles have a better detectability than the dipole in the high-SNR regime, because their ratio $\epsilon_{LM,\text{min}}/\epsilon_{LM,\text{max}}$ reaches a lower asymptotic value. For $\ell_{\text{max}} = 20$ the asymptotic value for the minimum quadrupole $\epsilon_{2M,\text{min}}$ (for any given M component) is just above the maximal $\epsilon_{2M,\text{max}} = \sqrt{4\pi/5}$, while for the overall quadrupole (defined similarly to Eq. 28) an amount as small as 0.45

times the maximal quadrupole can be detected. As for the dipole, also higher order multipoles reach the asymptotic regime only at very large SNR, of the order of $(SNR)_{high}$ defined in Eq. 27. It can be seen from Fig. 2 that, assuming $\ell_{\max} = 20$, when $SNR \lesssim 100$ (certainly including more realistic values of SNR) the dipole has the lower, and thus the best, value of $\epsilon_{LM,\min}/\epsilon_{LM,\max}$ for a single M component, although such SNR is not good enough for single M detections. For $\ell_{\max} = 10$ (corresponding to $N_p = 100$) and $SNR = 400$, which are the threshold values mentioned at the end of Section V B, an overall quadrupole equal to 0.72 times the maximal value is observable, and overall multipoles up to $L = 8$ and close to their respective maximal values can also be detected. Unless the isotropic signal SNR is increased to even more non-realistic values, the conclusions about detectability of dipole and higher multipoles presented here could be altered only with an exponentially large number of pulsars (or, as alluded to below, by co-adding multiple frequencies in the event that multiple frequencies have similar SNR).

VI. CONCLUSIONS

We have augmented prior work [29] to develop estimators and evaluate the detectability with PTAs of circular-polarization anisotropies in the stochastic GW background. We confirm with this new formalism earlier findings [30] that the circular-polarization monopole is not detectable. We evaluate the smallest detectable circular-polarization dipole anisotropy and find that its overall amplitude (i.e. without constraints to the direction) is conceivably detectable if it is close to maximal, if the isotropic signal is detected at the $\gtrsim 400\sigma$ level, and at least $N_p \sim 100$ pulsars are observed. In those conditions also a few higher overall multipoles can be detected. The results suggest an only logarithmic improvement in the sensitivity with the number of pulsars. A certain improvement can be obtained with increased overall signal, but it would be pushed to even more non-realistic values.

We have throughout assumed that the analysis was performed with just one frequency f, whereas in practice there may be many frequency channels available. The analysis can, however, be done individually for each available frequency and the results then added in quadrature. If the stochastic background is assumed to be uncorrelated at different frequencies, then the signal-to-noise with which a circular-polarization anisotropy can be detected will be the sum, in quadrature, of the signal-to-noise for each individual channel f. If these signal-to-noises are comparable for all of the available frequencies, then the SNR could conceivably be increased by a factor of the square root of the number of frequencies (a number of order 100 for 10 years of observations with a two-week cadence). In practice, though, the signal (the stochastic GW background) and noise are likely to have different frequency dependences, and if so, the overall SNR is dominated by only one, or perhaps a handful, of frequencies. In this case, the estimates of the detectability of the circular-polarization dipole (and higher moments) presented here might be improved, but probably by no more than a factor of a few.

On the other hand, we have considered an idealization of the measurements in which pulsars are roughly uniformly distributed on the sky and observed with comparable timing-residual noise. In practice, the distribution is not uniform, and the timing-residual noises vary from one pulsar to another. These complications are straightforward to deal with using techniques [30] already developed. These complications will, however, degrade the sensitivities to circular polarization relative to those obtained with the idealizations adopted here.

Finally, we have focussed here on the PTA characterization of a stochastic GW background. There is, however, a close correspondence between PTA searches and astrometry searches (see, e.g., Ref. [20]). Circular-polarization estimators for astrometry searches should thus be similarly obtained, and the quantitative conclusions about detectability similar. It may also be interesting in future work to investigate the possibility to co-add information on circular-polarization and intensity anisotropies that may arise if the local signal is due to a handful of nearby SMBH pairs.

[1] S. L. Detweiler, "Pulsar timing measurements and the search for gravitational waves," Astrophys. J. **234**, 1100 (1979).

[2] M. V. Sazhin, "Opportunities for detecting ultralong gravitational waves," Sov. Astron. **22**, 36 (1978).

[3] R. S. Foster and D. C. Backer, "Constructing a pulsar timing array," Astrophys. J. **361**, 300 (1990).

[4] M. Maggiore, "Gravitational wave experiments and early universe cosmology," Phys. Rept. **331**, 283 (2000) [gr-qc/9909001].

[5] S. Burke-Spolaor, "Gravitational-Wave Detection and Astrophysics with Pulsar Timing Arrays," arXiv:1511.07869 [astro-ph.IM].

[6] A. N. Lommen, "Pulsar timing arrays: the promise of

gravitational wave detection," Rept. Prog. Phys. **78**, no. 12, 124901 (2015).

[7] G. Hobbs and S. Dai, "Gravitational wave research using pulsar timing arrays," Natl. Sci. Rev. **4**, no. 5, 707 (2017) [arXiv:1707.01615 [astro-ph.IM]].

[8] N. Yunes and X. Siemens, "Gravitational-Wave Tests of General Relativity with Ground-Based Detectors and Pulsar Timing-Arrays," Living Rev. Rel. **16**, 9 (2013) [arXiv:1304.3473 [gr-qc]].

[9] G. Hobbs, "The Parkes Pulsar Timing Array," Class. Quant. Grav. **30**, 224007 (2013) [arXiv:1307.2629 [astro-ph.IM]].

[10] R. N. Manchester *et al.*, "The Parkes Pulsar Timing Array Project," Publ. Astron. Soc. Austral. **30**, 17 (2013) [arXiv:1210.6130 [astro-ph.IM]].

[11] Z. Arzoumanian *et al.* [NANOGRAV Collaboration], "The NANOGrav 11-year Data Set: Pulsar-timing Constraints On The Stochastic Gravitational-wave Background," Astrophys. J. **859**, no. 1, 47 (2018) [arXiv:1801.02617 [astro-ph.HE]].

[12] L. Lentati *et al.*, "European Pulsar Timing Array Limits On An Isotropic Stochastic Gravitational-Wave Background," Mon. Not. Roy. Astron. Soc. **453**, no. 3, 2576 (2015) [arXiv:1504.03692 [astro-ph.CO]].

[13] J. P. W. Verbiest *et al.*, "The International Pulsar Timing Array: First Data Release," Mon. Not. Roy. Astron. Soc. **458**, no. 2, 1267 (2016) [arXiv:1602.03640 [astro-ph.IM]].

[14] M. Rajagopal and R. W. Romani, "Ultralow frequency gravitational radiation from massive black hole binaries," Astrophys. J. **446**, 543 (1995) [astro-ph/9412038].

[15] A. H. Jaffe and D. C. Backer, "Gravitational waves probe the coalescence rate of massive black hole binaries," Astrophys. J. **583**, 616 (2003) [astro-ph/0210148].

[16] L. G. Book and E. E. Flanagan, "Astrometric Effects of a Stochastic Gravitational Wave Background," Phys. Rev. D **83**, 024024 (2011) [arXiv:1009.4192 [astro-ph.CO]].

[17] C. J. Moore, D. P. Mihaylov, A. Lasenby and G. Gilmore, "Astrometric Search Method for Individually Resolvable Gravitational Wave Sources with Gaia," Phys. Rev. Lett. **119**, no. 26, 261102 (2017) [arXiv:1707.06239 [astro-ph.IM]].

[18] D. P. Mihaylov, C. J. Moore, J. R. Gair, A. Lasenby and G. Gilmore, "Astrometric Effects of Gravitational Wave Backgrounds with non-Einsteinian Polarizations," Phys. Rev. D **97**, no. 12, 124058 (2018) [arXiv:1804.00660 [gr-qc]].

[19] L. O'Beirne and N. J. Cornish, "Constraining the Polarization Content of Gravitational Waves with Astrometry," Phys. Rev. D **98**, no. 2, 024020 (2018) [arXiv:1804.03146 [gr-qc]].

[20] W. Qin, K. K. Boddy, M. Kamionkowski and L. Dai, "Pulsar-timing arrays, astrometry, and gravitational waves," Phys. Rev. D **99**, no. 6, 063002 (2019) [arXiv:1810.02369 [astro-ph.CO]].

[21] B. Allen and A. C. Ottewill, "Detection of anisotropies in the gravitational wave stochastic background," Phys. Rev. D **56**, 545 (1997) [gr-qc/9607068].

[22] A. Sesana, A. Vecchio and M. Volonteri, "Gravitational waves from resolvable massive black hole binary sys-

tems and observations with Pulsar Timing Arrays," Mon. Not. Roy. Astron. Soc. **394**, 2255 (2009) [arXiv:0809.3412 [astro-ph]].

[23] V. Ravi, J. S. B. Wyithe, G. Hobbs, R. M. Shannon, R. N. Manchester, D. R. B. Yardley and M. J. Keith, "Does a 'stochastic' background of gravitational waves exist in the pulsar timing band?," Astrophys. J. **761**, 84 (2012) [arXiv:1210.3854 [astro-ph.CO]].

[24] N. J. Cornish and A. Sesana, "Pulsar Timing Array Analysis for Black Hole Backgrounds," Class. Quant. Grav. **30**, 224005 (2013) [arXiv:1305.0326 [gr-qc]].

[25] L. Z. Kelley, L. Blecha, L. Hernquist, A. Sesana and S. R. Taylor, "Single Sources in the Low-Frequency Gravitational Wave Sky: properties and time to detection by pulsar timing arrays," Mon. Not. Roy. Astron. Soc. **477**, no. 1, 964 (2018) [arXiv:1711.00075 [astro-ph.HE]].

[26] M. Anholm, S. Ballmer, J. D. E. Creighton, L. R. Price and X. Siemens, "Optimal strategies for gravitational wave stochastic background searches in pulsar timing data," Phys. Rev. D **79**, 084030 (2009) [arXiv:0809.0701 [gr-qc]].

[27] C. M. F. Mingarelli, T. Sidery, I. Mandel and A. Vecchio, "Characterizing gravitational wave stochastic background anisotropy with pulsar timing arrays," Phys. Rev. D **88**, no. 6, 062005 (2013) [arXiv:1306.5394 [astro-ph.HE]].

[28] J. Gair, J. D. Romano, S. Taylor and C. M. F. Mingarelli, "Mapping gravitational-wave backgrounds using methods from CMB analysis: Application to pulsar timing arrays," Phys. Rev. D **90**, no. 8, 082001 (2014) [arXiv:1406.4664 [gr-qc]].

[29] S. C. Hotinli, M. Kamionkowski and A. H. Jaffe, "The search for anisotropy in the gravitational-wave background with pulsar-timing arrays," arXiv:1904.05348 [astro-ph.CO].

[30] R. Kato and J. Soda, "Probing circular polarization in stochastic gravitational wave background with pulsar timing arrays," Phys. Rev. D **93**, no. 6, 062003 (2016) [arXiv:1512.09139 [gr-qc]].

[31] A. Hajian and T. Souradeep, "Measuring statistical isotropy of the CMB anisotropy," Astrophys. J. **597**, L5 (2003) [astro-ph/0308001].

[32] A. Hajian and T. Souradeep, "The Cosmic microwave background bipolar power spectrum: Basic formalism and applications," astro-ph/0501001.

[33] N. Joshi, S. Jhingan, T. Souradeep and A. Hajian, "Bipolar Harmonic encoding of CMB correlation patterns," Phys. Rev. D **81**, 083012 (2010) [arXiv:0912.3217 [astro-ph.CO]].

[34] L. G. Book, M. Kamionkowski and T. Souradeep, "Odd-Parity Bipolar Spherical Harmonics," Phys. Rev. D **85**, 023010 (2012) [arXiv:1109.2910 [astro-ph.CO]].

[35] A. R. Pullen and M. Kamionkowski, "Cosmic Microwave Background Statistics for a Direction-Dependent Primordial Power Spectrum," Phys. Rev. D **76**, 103529 (2007) [arXiv:0709.1144 [astro-ph]].

[36] E. Roebber and G. Holder, "Harmonic space analysis of pulsar timing array redshift maps," Astrophys. J. **835**, no. 1, 21 (2017) [arXiv:1609.06758 [astro-ph.CO]].